HHS Public Access

Author manuscript

Mol Cancer Res. Author manuscript; available in PMC 2024 June 01.

Published in final edited form as:

Mol Cancer Res. 2023 December 01; 21(12): 1303–1316. doi:10.1158/1541-7786.MCR-23-0169.

FBXO24 suppresses breast cancer tumorigenesis by targeting LSD1 for ubiquitination

Bo Dong[1,2,†], **Xiang Song**[1,2,3,4,†], **Xinzhao Wang**[1,2], **Tao Dai**[1,2], **Jianlin Wang**[1,2], **Yu Zhiyong**[3], **Jiong Deng**[5], **B. Mark Evers**[3], **Yadi Wu**[1,2,*]

[1]Department of Pharmacology & Nutritional Sciences, Markey Cancer Center, the University of Kentucky, College of Medicine, Lexington, KY 40506, United States

[2]Markey Cancer Center, the University of Kentucky, College of Medicine, Lexington, KY 40506, United States

[3]Department of Oncology, Shandong Cancer Hospital Affiliated to Shandong University, Shandong Academy of Medical Sciences, Jinan, Shandong, People's Republic of China.

[4]First Clinical Medical College, Shandong University of Traditional Chinese Medicine, Jinan, Shandong, 250355, People's Republic of China.

[5]Medical Research Institute, Binzhou Medical University Hospital, Binzhou, China.

Abstract

LSD1, a critical chromatin modulator, functions as an oncogene by demethylation of H3K4me1/2. The stability of LSD1 is governed by a complex and intricate process involving ubiquitination and deubiquitination. Several deubiquitinases preserve LSD1 protein levels. However, the precise mechanism underlying the degradation of LSD1, which could mitigate its oncogenic function remains unknown. To gain a better understanding of LSD1 degradation, we conducted an unbiased siRNA screening targeting all the human SCF family E3 ligases. Our screening identified FBXO24 as a genuine E3 ligase that ubiquitinates and degrades LSD1. As a result, FBXO24 inhibits LSD1-induced tumorigenesis and functions as a tumor suppressor in breast cancer cells. Moreover, FBXO24 exhibits an inverse correlation with LSD1 and is associated with a favorable prognosis in breast cancer patient samples. Taken together, our study uncovers the significant role of FBXO24 in impeding breast tumor progression by targeting LSD1 for degradation.

Keywords

FBXO24; LSD1; ubiquitination; breast cancer; E3 ligase

[*]Correspondence: Yadi Wu, Associate Professor, Department of Pharmacology & Nutritional Sciences, 432 HKRB, 760 Press Avenue, Lexington, KY 40508, (859)323-4589, yadi.wu@uky.edu.

[†]These authors contributed equally to this work.

Author Contributions: B.D., X. S., X.W., T.D., J.W., acquired and analyzed the data. Y.L., Z.Y., J.D., BM Evers provided reagents or contributed to experimental design and manuscript preparation. Y. W. supervised the study design, prepared the manuscript, and provided project leadership.

The authors declare no potential conflicts of interest.

Introduction

Histone-modifying enzymes play a central role in controlling gene expression, and the dysregulated expression of these enzymes significantly contributes to the initiation, progression, and metastasis of tumors[1,2]. Lysine-Specific Demethylase 1 (LSD1), the first identified histone demethylase that specifically remove H3K4 methylation, acts as a critical regulator of tumor initiation and progression[3–5]. LSD1 functions as an epigenetic regulator primarily through an amine oxidase reaction, targeting the removal of H3K4 mono-/di-methylation, an activation marker of transcription[6,7]. Elevated levels of LSD1 have been observed in leukemia, non-small cell lung, pancreatic, prostate, and breast cancers[5,8–10]. Overexpression of LSD1 is associated with tumor aggressiveness, metastasis, recurrence, and drug resistance and serve as a biomarker of poor prognosis[11,12]. LSD1 participates in various protein complexes that modulate distinct molecular targets involved in epithelial-mesenchymal transition (EMT), metastasis and the generation of cancer stem cells (CSC)s across different malignancies [13–17]. For example, our research demonstrated that LSD1 interacts with Snail1 and promotes breast cancer metastasis by downregulation of CDH1[18]. Furthermore, recent studies have indicated that inhibiting LSD1 enhances the efficacy of antitumor therapies, including immunotherapy[19,20].

LSD1 is regulated at both transcriptional and post-translational levels. Several studies including ours, have demonstrated that LSD1 is tightly controlled by the ubiquitin-proteasome system (UPS)[9,18,21,22]. Our recent findings have revealed that USP28 acts as the deubiquitinase for LSD1, leading to its stabilization[22]. In addition, other deubiquitinases such as USP22, USP7 and OTUD7B have also been reported to contribute to LSD1 stability[9,23,24]. However, the *bona fide* E3 ligase responsible for LSD1 degradation remains largely unknown. It is worth noting that LSD1 harbours canonical (I/L)Q motifs, which are typically recognized and ubiquitinated by F-box protein[25]. Therefore, it is plausible that the ubiquitination of LSD1 is mediated by an E3 ligase belonging to the F-box protein family. F-box proteins are categorized into three subfamilies: F-box and WD40 domain (FBXW), F-box and leucine-rich repeat (FBXL), and F-box and other domains (FBXO)[26]. One member of the F-box protein family, FBXO24, is an evolutionarily conserved chromatin-binding protein[27,28]. Previous studies have shown that FBXO24 contributes to ubiquitination and proteasomal degradation of protein arginine methyltransferase 6 (PRMT6), a co-regulator of gene expression that methylates histone H3 on arginine 2(H3R2), H4R3 and H2AR3 [29]. These findings suggest that FBXO24 plays a crucial role in modulating chromatin modification enzymes. However, the underlying mechanism of FBXO24-mediated protein degradation through the UPS, as well as the full extent of FBXO24's function, remains unexplored.

In this study, we conducted mechanistic investigations that unveiled the role of SCF-FBXO24 as an E3 ubiquitin ligase responsible for the ubiquitination and degradation of LSD1. Our findings demonstrated that FBXO24 interacts with LSD1 and mediates its degradation. We further confirmed this by observing that knockout of FBXO24 prevented LSD1 degradation. On the contrary, overexpression of FBXO24 led to the inhibition of breast cancer tumorigenesis, including suppression of proliferation, modulation of CSC

properties, inhibition of tumor invasion and metastasis, and prevention of immune evasion. These results collectively establish a previously unknown mechanism for LSD1 degradation and highlight the crucial function of FBXO24 as a tumor suppressor in the control of breast cancer tumor progression.

Materials and Methods

Cell Culture

All cell lines were purchased from the American Type Culture Collection (Manassas, VA). The human embryonic kidney HEK293, breast cancer MDA-MB-468, MDA-MB-231, MDA-MB-436, HS 578T, MCF7, MDA-MB-453 and MDA-MB-157 cell lines were grown in Dulbecco's modified Eagle's/F12 medium plus 10% fetal bovine serum as described previously[18]. The breast cancer cell lines T-47D, ZR-75-1, BT474, and HCC1937 were grown in RPMI1640 plus 10% FBS. All the cells lines were routinely checked for morphological and growth changes to probe for cross-contaminated, or genetically drifted cells. If any of these features occurred, we use the Short Tandem Repeat profiling service by ATCC to re-authenticate the cell lines. In addition, all cell lines were routinely checked for mycoplasma every 6 months. Cells were used within 20 passages.

Small Interfering RNA (siRNA) library Screening

The human E3 ubiquitin ligase siARRAY RTF was purchased from Dharmacon (Chicago, IL). The screen was performed according to manufacturer's instructions. In brief, the cells were added to rehydrated Dharmacon RTF siRNA library plates. Two days later, the cell lysates were extracted and the expression of LSD1 was detected by western blot.

Plasmids and Reagents

Plasmids of wild-type and deletion mutants for LSD1 were generated as described[18]. To generate Myc-FBXO24 constructs, FBXO24 cDNAs were amplified by PCR and subcloned into the lentiviral vector pLenti6.3/V5-Topo. To generate various Myc-FBXO24 deletion truncations, the constructs of FBXO24 cDNA were amplified by PCR and cloned into pCMV-3Tag. To generate various GST-FBXO24 deletion constructs, FBXO24 cDNAs were amplified by PCR and then subcloned into the pGEX-6P-1 expression vector. Site-directed mutagenesis Flag-LSD1 mutant were generated using a QuikChange II XL Site-Directed Mutagenesis Kit (Stratagene). All constructs were verified by sequence analysis (HuaGene Biotech). The FBXO24 guided RNA (gRNA) was designed using an online tool (https://portals.broadinstitute.org/gpp/public/maintenance?rp=/analysis-tools/sgrna-design) and subcloned into lentiCRISPRV2. Lentivirus was produced by co-transfecting 293T cells with pMD2.G, pMDLg/pRRE, and LentiCRISPRV2 or pLenti-puro expression vectors. Culture supernatants containing viral particles were collected 48 h after transfection. Cancer cells were infected with lentivirus and selected by puromycin 48h after infection. All the antibodies used in this study are listed in Supplemental table 1.

In vivo Ubiquitination Assay

HEK293 cells were transfected with HA-ubiquitin, Flag-LSD1 and Myc-FBXO24 plasmids as indicated. The cells were treated for 6 h with 10 μM MG132 at 48 h post-transfection, and then lysed. The samples were immunoprecipitated using anti-Flag agarose (Sigma).

GST Pull-down Assay

Glutathione-*S*-transferase proteins were expressed as described previously[30]. Cells were subjected to lysis in GST pull-down buffer (20 mM Tris, 150 mM NaCl and 1% Nonidet P-40 with protease cocktail) and rotated with glutathione–Sepharose-bound wild-type or deletion mutants of GST–LSD1. The binding complexes were eluted with SDS–PAGE sample buffer. About one-tenth of these eluents were analyzed for the association of FBXO24 or LSD1 by western blot and the remainder of the lysates were examined for the presence of purified GST–LSD1 or GST-FBXO24 by Coomassie staining.

Immunoprecipitation and Western Blot Analysis

Immunoprecipitation (IP) and western blot analysis were performed as described[31]. In brief, cells were lysed by IP buffer (25 mM Tris (pH 7.4), 150 mM NaCl, 5 μg/ml aprotinin, 1 μg/ml pepstatin, 1% Nonidet P-40, 1 mM EDTA and 5% glycerol). Cell lysates were incubated with antibodies conjugated to agarose beads overnight at 4°C. The beads were then rinsed with IP buffer, and the immunoprecipitated protein complexes were subjected to western blot analysis. For western blot analysis, cultured cells were lysed in buffer (50 mM Tris (pH 7.5), 150 mM NaCl, 5 μg/ml aprotinin, 1 μg/ml pepstatin, 1% Nonidet P-40, 1 mM EDTA and 0.25% deoxycholate). Equal amounts of protein extracts were resolved by 10% SDS–PAGE, and then transferred to a PVDF membrane (Millipore). The membrane was probed with primary antibodies, followed by second antibodies conjugated to horseradish peroxidase. Quantitative densitometry analysis was employed with image analysis software. The antibodies were shown in the Supplemental table 1

Chromatin Immunoprecipitation (ChIP)

Chromatin immunoprecipitation assays were performed using the Imprint Chromatin Immunoprecipitation kit (Sigma) according to the manufacturer's instructions. Briefly, cells were cross-linked with 1% formaldehyde at room temperature for 10 min and the cross-link was quenched by 125 mM glycine. Cells were lysed with L1 buffer (50 mM Tris, 2 mM EDTA, 0.1% IGEPAL, 10% glycerol, 1 mM dithiothreitol, 1 mM phenylmethylsulfonyl fluoride (PMSF) and protease inhibitor mixture, pH 8.0) on ice. Chromatin was fragmented by using micrococcal nuclease (MNase) digestion. Fragmented chromatin was incubated with antibodies and protein-G magnetic beads at 4°C overnight. Bound DNA-protein complexes were washed, eluted, and de-crosslinked. Purified DNA was resuspended in TE buffer (10 mM Tris-HCL and 1 mM EDTA, pH 8.0) for ChIP-seq and PCR. Signals were validated by real-time PCR using SYBR Green Power Master Mix following the manufacturer's protocol (Applied Biosystems). The sequence of primers was listed in Supplemental table 2

Immunofluorescence Staining

The immunofluorescence staining was performed as described[31]. Briefly, cells were seeded on cover slips. Then, cells were fixed with 4% paraformaldehyde and subsequently incubated with anti-FBXO24 and anti-LSD1 antibodies at 4°C overnight. The cells were further incubated with goat anti-mouse conjugated with Alexa fluor 568 and goat-anti-rabbit conjugated with Alexa fluor 488, respectively (Invitrogen, Carlsbad, CA). Finally, nuclei were counterstained with 4′, 6′-diamidino-2-phenylindole (Sigma-Aldrich) for 20 min and images were taken by a fluorescent microscope.

Immunohistochemical (IHC) Staining

Breast cancer TMA was purchased from Pantomics (BRC2281). 30 formalin-fixed paraffin-embedded (FFPE) samples of lymph node metastases were collected from breast cancer patients at our institute with the approval of the Institutional Review Board (IRB). Sections were deparaffinized with xylene, hydrated using a diluted alcohol series, and treated in 3% H_2O_2 in methanol to quench endogenous peroxidase activity. Tissue samples were stained with anti-FBXO24 (OriGene) and anti-LSD1 (Abcam) antibodies, and each sample was scored by the H-score method that combines the values of immunoreaction intensity and the percentage of tumor cell staining as described previously[32]. Briefly, the IHC staining was scored according to the following criteria: negative: 0–10% of the cells stained; low: 10–40% stained; and High: 40–100% stained. All slides were independently evaluated by two investigators. Chi-square analysis was used to analyze the relationship between FBXO24 and LSD1 expression; statistical significance was defined as $P<0.05$. The antibodies were shown in the Supplemental table 1. Data regarding the stage and expression of ERα, PR, and HER2 for FFPE sample was presented in Supplemental table 4.

Histone Acid Extraction

Cell pellets were resuspended in PBS with 0.5% TritonX-100 and rotated for 10 min. The lysate was centrifuged to spin down the nuclei. The pellet was washed once in the extraction buffer and then re-suspended in 0.2 N HCl overnight at 4°C on a rotator. The lysate was then centrifuged and the supernatant was quantified.

Quantitative Real-Time PCR

Total RNA was isolated using the RNeasy Mini kit (Qiagen) according to the manufacturer's instructions. Specific quantitative real-time PCR experiments were performed using SYBR Green Power Master Mix following manufacturer's protocol (Applied Biosystems). The results were normalized to *ACTB* mRNA. The sequence of primers was listed in Supplemental table 2

Fluorescence-Activated Cell Sorting (FACS)

Cells were detached from plates and incubated with anti-human CD44 and anti-human CD24 (PE-conjugated, ebioscience), and finally analyzed using a FACSCalibur flow cytometer.

Tumorsphere-formation Assay

Tumorsphere cultures were performed as described in Dontu et al [33]. In brief, cell monolayers were plated as single-cell suspensions on ultra-low attachment plates (Corning) in DMEM/F12 medium supplemented with 20 ng/ml EGF, 10 μg/ml insulin, 0.5 μg/ml hydrocortisone and B27. Tumorspheres were counted via visual inspection after 5–10 days.

Luciferase Reporter Assay

Luciferase assays were performed as described previously[32]. Briefly, cells were grown to 50% confluence in 6-well dishes and then co-transfected to include the *CDH1* promoter luciferase reporter, vector or FBXO24, along with LSD1-3KR in each well using Fugene 6 (Roche, Indianapolis, IN). To normalize transfection efficiency, cells were also co-transfected with 0.1 μg of the pRL-CMV (Renilla luciferase). Luciferase activity was measured using the Dual-Luciferase Assay kit (Promega, Madison, WI). Three independent experiments in triplicates were performed, and the calculated means and standard deviations are presented.

Wound-healing, invasion and migration Assay

The wound-healing assay was performed as described[31]. Briefly, cells were grown in 6-well plates. The wound was created by 1 mL pipet tips when cells became confluence. The culture medium was replaced by medium containing 0.1% FBS. Images were taken at the indicated time points, and the wound closure ratios were calculated after 24 h. Invasion and migration assays were performed in Boyden chambers coated with (invasion) or without Matrigel (Migration) as instructed by the manufacturer (BD biosciences)[31]. Cancer cells were plated in the upper chamber, serum-free culture medium plus 100 nM lysophosphatidic acid was added in the bottom chamber as a chemoattractant. The invasive cancer cells were stained with crystal violent. Cells were counted with an inverted microscope. All experiments were performed in triplicate.

Cell viability and colony-formation

CCK8 proliferation assays (Takala, Japan) were performed to determine the effect of FBXO24 on proliferation[34]. Transfected cells were grown in 96-well plates in triplicate. At indicated time points, 10μL CCK-8 solution was added and incubated for 2–4h. The staining intensity was measured as an absorbance 450nm. Results are presented as the means ± standard deviation (SD). Data were based on three independent experiments. For colony-formation analysis, cells were plated in 6-well plates (2,000 cells/well) in triplicate. After 2 weeks, colonies were washed with PBS, fixed in methanol, stained with 0.1% crystal violet, and counted using an inverted microscope.

In vivo Tumorigenesis Assay

Female ICR-SCID mice (6–8 wks old) were purchased from Taconic (Germantown, NY) and maintained and treated under specific pathogen-free conditions. All procedures were approved by the Institutional Animal Care and Use Committee at the University of Kentucky College of Medicine and conform to the legal mandates and federal guidelines for the care and maintenance of laboratory animals. Mice were injected with the breast

cancer MDA-MB-231-luciferase cell line and corresponding stable clones with FBXO24 or FBXO24+LSD1-3KR expression (2×10^6 cells/mouse, 6 mice/group) via mammary fat pad injection. Tumor growth was monitored with caliper measurements. When tumors were approximately 1.0 cm in size, mice were euthanized and tumors were excised. Data were analyzed using the Student's t-test; a p value <0.05 was considered significant.

Patient Samples

With the Institutional Review Board (IRB) permission[35], 12 frozen fresh tumor samples were obtained from patients' resected breast tumors at our facility. In Supplemental table 3, information on the stage, grade, and expression of ERα, PR, and HER2 was shown. These samples were "snap-frozen" in liquid nitrogen. Hematoxylin and eosin (H&E) stained tissue slices were used for the histological examination of each sample. Tumor samples regions were microscopically dissected and evaluated. The investigation was limited to samples that consistently contained more than 75% tumor cells in the tissues. The samples were homogenized using a Dounce homogenizer in homogenizer buffer then re-suspended in lysis buffer after centrifugation and processed for western blot.

Statistical analysis

The statistical analysis was performed as described[31]. All data are presented as the mean ± standard error from at least three independent experiments. The Student *t* test was used to compare data between two groups. Survival curves were obtained using the Kaplan–Meier method, and the log-rank test was used to test the difference in survival curves. Multivariate analysis was performed using the Cox's regression multiple hazard model. *P* values of less than 0.05 were considered statistically significant.

Result

FBXO24 is a bona fide E3 ligase that targets the degradation of the LSD1 protein.

Since LSD1 harbors an F-box recognition motif[25], we focused on genes that encode F-box containing proteins as potential sources of the E3 ligases. We conducted a screening using western blot analysis and an E3 ligase siRNA library from Dharmacon (subset 2). This library includes siRNAs against all SOCS-box and F-box-containing proteins. The positive hits from the screening were further validated using three different siRNAs against the specific F-box gene under investigation. The interactions between these E3 candidates and LSD1 were also confirmed through co-immunoprecipitation (Co-IP) experiments. Out of the 68 genes encoding F-box proteins that were screened, we identified one potential positive hit, which was FBXO24 (Fig. 1A). To validate these findings, we screened a panel of human F-box proteins and determined that FBXO24 was the only E3 ligase capable of reducing LSD1 expression (Fig. 1B). Moreover, the expression of LSD1 decreased in a dose-dependent manner upon ectopic expression of FBXO24 (Fig. 1C). To further establish the specificity of FBXO24 as the ubiquitin E3 ligase for LSD1, we generated a deletion mutant of FBXO24 that lacks the F-box domain (ΔF-FBXO24). Overexpression of the wild-type (WT) FBXO24 resulted in decreased LSD1 expression, whereas the ΔF-box mutant construct failed to exhibit this effect (Fig. 1D). Additionally, we observed a specific increase in the levels of LSD1 protein in FBXO24 CRISPR knockout MDA-MB-436 and HS 578T

cells using two different guided RNAs (Fig. 1E). In contrast, when we overexpressed FBXO24 in T-47D, MDA-MB-468, and MDA-MB-231 cells, which naturally have low levels of endogenous FBXO24 but abundant LSD1, we observed a significant increase in LSD1 protein degradation with no change in mRNA levels (Fig. 1F and Supplemental Fig. 1A). Because LSD1 is a major demethylase for H3K4me2, we examined the global levels of H3K4me2 with ectopic FBXO24 expression and observed a significant increase in H3K4me2 levels upon overexpression of FBXO24 (Fig. 1G). However, it is important to note that the levels of H3K9me2 remained unaffected by ectopic FBXO24 expression. These findings collectively indicate that FBXO24 plays a role in the regulation of LSD1 degradation and that this regulation relies on the intact E3 ligase function of FBXO24.

FBXO24 interacts with LSD1.

We initially investigated the expression of FBXO24 and LSD1 in multiple breast cancer cell lines (Fig. 2A). Interestingly, we observed that LSD1 was highly expressed in most breast cancer cell lines that exhibited low levels of FBXO24 expression. This correlation between low FBXO24 and high LSD1 expression was also evident in lung cancer (Supplemental Fig. 1B). However, we did not find a significant correlation between LSD1 and Jade2, a previously reported E3 ligase of LSD1. Additionally, the knockdown of Jade2 did not have any discernible effect on the stability of LSD1 (Supplemental Fig. 1C). These findings suggest that the regulation of LSD1 stability is specifically mediated by FBXO24 rather than Jade2.

To investigate the interaction between FBXO24 and LSD1, we conducted co-expression experiments using Flag-LSD1 and Myc-FBXO24 in HEK293 cells. Immunoprecipitation of FBXO24 using a Myc antibody revealed the presence of associated LSD1, and vice versa when immunoprecipitated with Flag (Fig. 2B). Furthermore, we observed that endogenous FBXO24 co-precipitated with endogenous LSD1, especially after treating the cells with MG132 to prevent protein degradation (Fig. 2C). To further corroborate the interaction between FBXO24 and LSD1, we utilized confocal microscopy. When FBXO24 was co-expressed with GFP-LSD1 in HEK293 cells, we observed their co-localization in the nucleus (Fig. 2D). Additionally, we found that endogenous FBXO24 and LSD1 co-localized in the nucleus after treatment with MG132 (Fig. 2E).

The N-terminal one-third of LSD1 contains a SWIRM domain that is commonly found in chromatin remodeling complexes (Fig. 2F)[36]. The C-terminal two-thirds of LSD1 contain an amine oxidase (AO) domain that exhibits significant sequence similarity to FAD-dependent amine oxidase[18,36]. To identify the specific region responsible for the interaction between LSD1 and FBXO24, we generated LSD1 domain-deletion mutants and co-expressed them with FBXO24 in HEK293 cells. Co-IP experiments revealed that the interaction between LSD1 and FBXO24 required the AO domain of LSD1, whereas the SWIRM domain was dispensable for this interaction (Fig. 2F). We further confirmed this interaction using GST-pull down assays (Fig. 2G). To elucidate the region in FBXO24 that associates with LSD1, we generated several deletion mutants of FBXO24 and co-expressed them with LSD1 in HEK293 cells. Our findings indicated that the N-terminal region of FBXO24 retained the ability to interact with LSD1 (Fig. 2H). In contrast, the RCC1 domain

and F-box domain in the C-terminal region of FBXO24 were not required for the interaction with LSD1. Consistent with these results, GST-pull down assays provided additional confirmation that the N-terminal region of FBXO24 is essential for their interaction (Fig. 2I). Collectively, these data demonstrate a direct interaction between FBXO24 and LSD1, with the AO domain of LSD1 and the N-terminal region of FBXO24 mediating this interaction.

FBXO24 ubiquitinates LSD1.

To further investigate the role of FBXO24 in regulating the stability of LSD1, we assessed the protein half-life of LSD1 under different FBXO24 manipulations in the presence of cycloheximide (CHX) to block newly synthesized protein. Co-expression of Flag-LSD1 with myc-FBXO24 in HEK293 cells led to a rapid degradation and instability of LSD1 in the presence of FBXO24 (Fig. 3A). In contrast, FBXO24 CRISPR knock-out MDA-MB-436 cells exhibited stabilized levels of LSD1 (Fig. 3B). To determine whether FBXO24 promotes the ubiquitination of LSD1 for enhanced degradation, we co-transfected HEK293 cells with HA-ubiquitin (Ub), Myc-FBXO24 (wild type or ΔF-box mutant), and Flag-LSD1. Cells were treated with MG132 to prevent protein degradation before conducting a ubiquitination assay. The results showed a significant increase in polyubiquitinated LSD1 in cells transfected with FBXO24, while the ΔF-box mutant failed to induce LSD1 ubiquitination. This indicates that the ligase activity of FBXO24 is dependent on the integrity of the E-box domain (Fig. 3C). Furthermore, FBXO24 was found to promote the polyubiquitination of endogenous LSD1 (Fig. 3D).

To identify the lysine residues within LSD1 that undergo ubiquitination in vivo, we co-expressed FBXO24 with different LSD1 domains. Our findings suggested that the AO domain of LSD1 is responsible for its ubiquitination (Supplemental Fig. 2). Based on potential ubiquitination sites, we generated LSD1 mutants with single or multiple lysine-to-arginine (KR) substitutions in each potential ubiquitination site. Through these experiments, we identified that lysine residues K424/K432 and K481 are key sites for LSD1 ubiquitination (Fig. 3E). Subsequently, we generated a mutant (LSD1-3KR) in which these three lysine residues were replaced with alanine. Western blot analysis revealed that the 3KR mutant exhibited increased stability compared to wild-type LSD1 in the presence of FBXO24 (Fig. 3F). Consistently, *in vivo* ubiquitination studies demonstrated that the LSD1-3KR mutant was less ubiquitinated than the wild-type LSD1 (Fig. 3G). These findings collectively indicate that FBXO24 functions as a bona fide E3 ligase that promotes the ubiquitination and subsequent degradation of LSD1, resulting in a shortened protein half-life for LSD1.

FBXO24 represses tumorigenesis through LSD1 degradation.

To investigate the crucial role of FBXO24-mediated LSD1 degradation, we ectopically expressed FBXO24 and LSD1-3KR either alone or in combination in MDA-MB-231, MDA-MB-468, and T-47D cells. Cell proliferation analysis revealed that the ectopic expression of FBXO24 led to significant cell growth retardation compared to the control group (Fig. 4A). Furthermore, colony formation assays confirmed that overexpression of FBXO24 resulted in a reduction in colony numbers compared to the control group (Fig. 4B & C). Since LSD1

selectively promotes breast CSCs [9,16,37,38], we extended our investigation to assess the critical role of FBXO24 in regulating CSC-like properties in human breast cancer cells. We evaluated tumorsphere formation in cells expressing FBXO24. Our findings demonstrated that ectopic expression of FBXO24 markedly reduced the number and size of tumorspheres compared to the control group in MDA-MB-231, MDA-MB-468, and T-47D cells (Fig. 4D & E). This function of FBXO24 is likely mediated through the regulation of LSD1 since the expression of the degradation-resistant LSD1-3KR mutant rescued the expression and functional effects of LSD1. In addition to the functional assays mentioned earlier, we also examined the $CD44^{high}/CD24^{low}$ CSC population in the three cell lines (MDA-MB-231, MDA-MB-468, and T-47D) using fluorescence-activated cell sorting (FACS). We observed that ectopic expression of FBXO24 led to a reduction in the $CD44^{high}/CD24^{low}$ CSC population compared to the control group in all three cell lines (Fig. 4F). Notably, the reduction in the CSC population caused by FBXO24 expression could be restored by co-expression of the LSD1-3KR mutant, emphasizing the dependence on FBXO24-mediated LSD1 degradation. Consistent with the pivotal role of the FBXO24-LSD1 axis in regulating CSC-like characteristics, the ectopic expression of FBXO24 resulted in decreased expression of stem cell markers SOX2 and OCT4, while increasing the expression of the differentiation marker CDKN1A, at both mRNA and protein levels compared to the control group (Fig. 4G & H). Once again, the restoration of LSD1 expression rescued these changes in marker expression. These findings collectively indicate that the functional activities suppressed by FBXO24 require the degradation of LSD1, as demonstrated by the impaired effects observed upon ectopic expression of the LSD1-3KR mutant (Fig. 4).

FBXO24 expression inhibits EMT while promoting chemokine expression via degradation of LSD1.

It has been reported by our team and others that LSD1 enhances EMT-mediated cancer progression[18]. To investigate whether FBXO24 inhibits EMT, we measured the expression of EMT markers. We observed that FBXO24 expression led to the upregulation of epithelial markers such as E-cadherin and Claudin, while downregulating mesenchymal molecules including Vimentin compared to the control group. Concurrently, we observed the degradation of LSD1 (Fig. 5A & B). Immunofluorescence (IF) staining further confirmed that FBXO24 expression increased the levels of the epithelial marker E-cadherin, while decreasing N-cadherin and Vimentin levels (Fig. 5C). Consistent with the upregulation of E-cadherin, FBXO24 expression enhanced the promoter activity of CDH1 (the gene encoding E-cadherin) (Fig. 5D) and increased the levels of the permissive histone modification H3K4me2 in the *CDH1* promoter region (Fig. 5E). To assess the functional consequences of FBXO24 expression, we evaluated cell migration and invasiveness. FBXO24 expression significantly decreased cell migration and invasive capacity compared to the control group (Fig. 5F–K, Supplemental Fig. 3). Importantly, these functional activities inhibited by FBXO24 required LSD1 degradation, as exogenous expression of the LSD1-3KR mutant greatly rescued the effects of FBXO24 on EMT (Fig. 5, Supplemental Fig. 3).

Recent studies have provided evidence that LSD1 represses the expression of certain endogenous retroviral elements (ERV) and epigenetically silences the expression of chemokines involved in effector T cell function, such as CCL5 and CXCL10[19,20].

Interestingly, in our study, we found that FBXO24 expression induced the upregulation of ERVs and chemokine expression (Fig. 6A). This suggests that FBXO24 may counteract the repressive effects of LSD1 on ERVs and chemokines. To further investigate the mechanism underlying the FBXO24-induced expression of chemokines, we examined whether changes in H3K4me2 levels occurred at specific gene promoters. We observed that FBXO24 expression enhanced the occupancy of H3K4me2 at distant regions upstream of the transcription start sites (TSS) of the *CCL5, CXCL9*, and *CXCL10* promoters (Fig. 6B). Once again, the reconstitution of LSD1-3KR significantly, although partially, rescued the effect of FBXO24 on chemokine expression (Fig. 6A & B). This suggests that the increase in chemokine expression is, at least in part, due to LSD1 degradation and subsequent alterations in histone methylation. Overall, these findings suggest that FBXO24 expression leads to the inhibition of EMT and upregulation of ERVs and chemokines, potentially counteracting the repressive effects of LSD1.

FBXO24 inhibits breast cancer cell proliferation in vivo and FBXO24 levels inversely correlate with LSD1 levels in tumor samples.

To directly assess the inhibitory effect of FBXO24 on tumor proliferation *in vivo*, we implanted MDA-MB-231-luciferase cells expressing FBXO24 into the mammary fat pad of female SCID mice and monitored tumor growth using bioluminescent imaging. After approximately 35 days, all control mice developed tumors, as shown in Figure 7A–D. However, to our surprise, mice injected with FBXO24-expressing cells did not exhibit any tumor formation. This observation is consistent with the *in vitro* function of LSD1, as LSD1-3KR cells displayed remarkable resistance to tumor growth suppression upon FBXO24 expression (Fig. 7A–D).

To further investigate the relationship between FBXO24 and LSD1 in human breast cancer, we analyzed the protein levels of FBXO24 and LSD1 in 12 fresh-frozen breast tumor samples. In most of these samples, with the exception of one (sample 4), we observed an inverse correlation between FBXO24 and LSD1 protein levels (Fig. 7E). To assess the clinical relevance of this relationship, we performed immunohistochemistry (IHC) staining on a breast cancer tissue microarray (TMA). The results revealed a strong inverse correlation between FBXO24 and LSD1, with prominent staining of LSD1 in the breast cancer tissues (Fig. 7F). Notably, FBXO24 expression was rarely detected in 90% of the breast cancer tumors. We further validated these findings in lymph node metastasis samples, which exhibited similar results to the TMA (Supplemental Fig. 4). Additionally, we observed lower expression of FBXO24 in multiple cancer tissues compared to normal tissues in the TCGA dataset (Fig. 7G). Interestingly, high expression of FBXO24 showed a significant negative association with tumor stage (Supplemental Fig. 5A). Considering that LSD1 has been identified as a marker for poor prognosis, with high expression correlating with worse outcome[11,12], we hypothesized that the E3 ligase(s) targeting LSD1 might indicate a favorable prognosis. We found that the expression of FBXO24 was positively correlated with improved patient survival in the TCGA dataset, including breast cancer (Supplemental Fig. 5B). Furthermore, we confirmed this correlation in various breast cancer gene expression datasets (Fig. 7H). Moreover, patients with low FBXO24 expression displayed a higher rate of relapse and lower 5-year survival in breast cancer

dataset (Supplemental Fig. 6A&B). Further analysis of the breast cancer dataset revealed a negative correlation between downregulation of FBXO24 expression and tumor grade and aggressiveness (Supplemental Fig. 6C&D). Collectively, these findings underscore the clinical relevance of the dysregulated FBXO24-LSD1 axis and emphasize the tumor-suppressive role of FBXO24 in tumor progression.

Discussion

LSD1 is a pivotal epigenetic regulator known for its involvement in various critical aspects of cancer biology, such as EMT, metastasis, acquisition of CSC-like properties, metabolic reprogramming, tumor recurrence, and evasion of immunotherapy. Through our study, we have discovered that FBXO24 functions as a *bona fide* E3 ligase for LSD1. Moreover, FBXO24 acts as a tumor suppressor by inhibiting tumor progression, including EMT, metastasis, CSC-like properties, while promoting the expression of chemokines (Fig. 7I). In our in vitro experiments, we demonstrated that the tumor-suppressive function of FBXO24 could be restored by the expression of exogenous LSD1 that is resistant to degradation. Notably, we have also established a robust correlation between FBXO24 and LSD1 in multiple cancer cell lines and human breast tumor specimens, thereby confirming the regulatory relationship between these two proteins. These findings shed light on the critical and novel role of the FBXO24-LSD1 axis in carcinogenesis.

The stability of LSD1 is intricately regulated by the UPS. Ubiquitination and deubiquitination, comprising a complex network of regulatory processes, maintain the dynamic homeostasis of LSD1. While several deubiquitinase enzymes have been identified in this context[9,22,24], the E3 ligase-mediated ubiquitination of LSD1 has remained unclear. Previous studies have reported certain E3 ligases capable of targeting LSD1 for proteasomal degradation. However, none of these identified proteins were typical E3 ligases. For instance, although Jade2 was reported to function as an E3 ligase in destabilizing LSD1 during neurogenesis [39], this observation is subject to controversy and requires further validation. This is due to the fact that Jade2 is primarily a transcription factor, and the reported Jade2-mediated ubiquitination of LSD1 relies on the PHD zinc finger domain of Jade2, rather than the classical RING finger domain present in almost all E3 ubiquitin ligases [39,40]. More recently, it was reported that p62 targets LSD1 for proteasomal degradation in the nucleus [24]. Considering that LSD1 contains canonical (I/L)Q motifs that are typically recognized and ubiquitinated by F-box proteins [25], our investigation into the responsible E3 ligase focused on the SCF (Skp1-Cullin1-F-box protein) family. Given that there are approximately 70 genes encoding F-box-containing E3 ligases, we extensively screened the entire set in search of the responsible gene. Ultimately, our screening efforts led us to identify FBXO24 as the sole E3 ligase associated with LSD1 regulation.

FBXO24 is classified as a chromatin-binding F-box protein [27,28], and its substrates include not only LSD1 but also PRMT6. Both LSD1 and PRMT6 are essential enzymes involved in histone modifications, indicating that FBXO24 plays a crucial role in chromatin modification. Although the precise function of FBXO24 is not fully understood, existing evidence suggests that the loss of FBXO24 is closely associated with tumor development and progression. For instance, FBXO24 is located in the chromosomal region 7q22.1,

which frequently experiences loss of heterozygosity in human breast cancer [27]. Moreover, FBXO24 is identified as one of three candidate tumor suppressor genes for diffuse gastric cancer. Sanger exome sequencing has revealed germline truncations in FBXO24, highlighting the contribution of FBXO24 mutations to the oncogenesis process[41]. Consistent with this, genomic mutation databases indicate that FBXO24 is mutated in various tumor types, including breast, gastric, lung, skin cancers, lymphoma, with mutations spanning the entire coding region. Notably, significant mutations occur in the catalytic F-box domain of FBXO24 (data from COSMIC) [42]. In our study, we observed minimal expression of FBXO24 in breast cancer samples (Fig. 7). Correspondingly, we found that ectopic expression of FBXO24 markedly suppressed cell proliferation, CSC-like properties, EMT, and metastasis (Fig. 4 and Fig. 5). Remarkably, we observed that FBXO24 expression completely abolished tumor formation in vivo (Fig. 7A–D). Our findings strongly support the tumor-suppressive role of FBXO24.

While our study has revealed FBXO24 as a bona fide E3 ligase for LSD1, there are still several unanswered questions that warrant further investigation. Firstly, do FBXO24 abundance and subcellular localization vary during the cell cycle? As LSD1 levels fluctuate in a cell-cycle-dependent manner [43,44], it would be interesting to determine whether the protein levels of FBXO24 show an inverse correlation with the kinetics of LSD1 fluctuation. Specifically, investigating whether FBXO24 abundance or its subcellular localization changes during different phases of the cell cycle could provide insights into the regulatory mechanisms governing LSD1 degradation. Secondly, is FBXO24-mediated LSD1 degradation phosphorylation-dependent? Most substrates of SCF E3 ligases require prior phosphorylation before being targeted for degradation [45]. It is plausible that LSD1 undergoes phosphorylation prior to recognition by FBXO24. Interestingly, many cyclin-dependent kinase (CDKs) including CDK1 and CDK2 effectively phosphorylate LSD1[46,47]. However, overexpression of CDK1 and CDK2 have no effect on LSD1 stability although both of them interact with LSD1. Exploring the phosphorylation status of LSD1 and its impact on FBXO24-mediated degradation could provide mechanistic insights into the regulation of LSD1 stability. Finally, is the activity of FBXO24 also affected by DNA damage? LSD1 is recruited to sites of DNA damage within a short time and promotes the DNA damage response function [48]. The LSD1 protein was reduced significantly 60 min after DNA damage. Interestingly, FBXO24 is associated with DNA damage [49]. Investigating the role of FBXO24 in the DNA damage response and assessing its activity in the context of DNA damage could uncover additional functions of FBXO24 beyond its interaction with LSD1. Addressing these outstanding questions would significantly enhance our understanding of the intricate relationship between LSD1 and FBXO24, shedding light on the regulatory mechanisms and broader biological functions of this axis.

In summary, our study highlights the crucial role of FBXO24 as a master chromatin-binding E3 ligase in tumor progression and the regulation of LSD1 signaling. By identifying FBXO24 as a key regulator of LSD1, our findings offer valuable insights into the underlying mechanisms of LSD1 regulation.

Supplementary Material

Refer to Web version on PubMed Central for supplementary material.

Acknowledgments

We thank Drs. Cathy Anthony and Binhua Peter Zhou for critical reading and editing of this manuscript, and Donna Gilbreath for assistance with graphics. This research was supported by the Shared Resources of the University of Kentucky Markey Cancer Center (P30CA177558). This work was also supported by grants from NIH (P20GM121327 and CA230758) to Y Wu.

REFERENCES

1. Dawson MA, Kouzarides T. Cancer epigenetics: from mechanism to therapy. Cell 2012; 150: 12–27 [PubMed: 22770212]
2. Rodriguez-Paredes M, Esteller M. Cancer epigenetics reaches mainstream oncology. Nat Med 2011; 17: 330–9 [PubMed: 21386836]
3. Zheng YC, Ma J, Wang Z, Li J, Jiang B, Zhou W, et al. A Systematic Review of Histone Lysine-Specific Demethylase 1 and Its Inhibitors. Med Res Rev 2015:
4. Schenk T, Chen WC, Gollner S, Howell L, Jin L, Hebestreit K, et al. Inhibition of the LSD1 (KDM1A) demethylase reactivates the all-trans-retinoic acid differentiation pathway in acute myeloid leukemia. Nat Med 2012; 18: 605–11 [PubMed: 22406747]
5. Choi HJ, Park JH, Park M, Won HY, Joo HS, Lee CH, et al. UTX inhibits EMT-induced breast CSC properties by epigenetic repression of EMT genes in cooperation with LSD1 and HDAC1. EMBO reports 2015; 16: 1288–98 [PubMed: 26303947]
6. Goldberg AD, Allis CD, Bernstein E. Epigenetics: a landscape takes shape. Cell 2007; 128: 635–8 [PubMed: 17320500]
7. Shi Y, Lan F, Matson C, Mulligan P, Whetstine JR, Cole PA, et al. Histone demethylation mediated by the nuclear amine oxidase homolog LSD1. Cell 2004; 119: 941–53 [PubMed: 15620353]
8. Schulte JH, Lim S, Schramm A, Friedrichs N, Koster J, Versteeg R, et al. Lysine-specific demethylase 1 is strongly expressed in poorly differentiated neuroblastoma: implications for therapy. Cancer Res 2009; 69: 2065–71 [PubMed: 19223552]
9. Zhou A, Lin K, Zhang S, Chen Y, Zhang N, Xue J, et al. Nuclear GSK3beta promotes tumorigenesis by phosphorylating KDM1A and inducing its deubiquitylation by USP22. Nat Cell Biol 2016; 18: 954–66 [PubMed: 27501329]
10. Kozono D, Li J, Nitta M, Sampetrean O, Gonda D, Kushwaha DS, et al. Dynamic epigenetic regulation of glioblastoma tumorigenicity through LSD1 modulation of MYC expression. Proc Natl Acad Sci U S A 2015; 112: E4055–64 [PubMed: 26159421]
11. Hayami S, Kelly JD, Cho HS, Yoshimatsu M, Unoki M, Tsunoda T, et al. Overexpression of LSD1 contributes to human carcinogenesis through chromatin regulation in various cancers. Int J Cancer 2011; 128: 574–86 [PubMed: 20333681]
12. Lim S, Janzer A, Becker A, Zimmer A, Schule R, Buettner R, et al. Lysine-specific demethylase 1 (LSD1) is highly expressed in ER-negative breast cancers and a biomarker predicting aggressive biology. Carcinogenesis 2010; 31: 512–20 [PubMed: 20042638]
13. Ding J, Zhang ZM, Xia Y, Liao GQ, Pan Y, Liu S, et al. LSD1-mediated epigenetic modification contributes to proliferation and metastasis of colon cancer. Br J Cancer 2013; 109: 994–1003 [PubMed: 23900215]
14. Chen J, Ding J, Wang Z, Zhu J, Wang X, Du J. Identification of downstream metastasis-associated target genes regulated by LSD1 in colon cancer cells. Oncotarget 2017; 8: 19609–30 [PubMed: 28121627]
15. Feng J, Xu G, Liu J, Zhang N, Li L, Ji J, et al. Phosphorylation of LSD1 at Ser112 is crucial for its function in induction of EMT and metastasis in breast cancer. Breast cancer research and treatment 2016; 159: 443–56 [PubMed: 27572339]

16. Wu Y, Zhou BP. Epigenetic regulation of LSD1 during mammary carcinogenesis. Mol Cell Oncol 2014; 1: e963426 [PubMed: 27308339]
17. Ambrosio S, Sacca CD, Majello B. Epigenetic regulation of epithelial to mesenchymal transition by the Lysine-specific demethylase LSD1/KDM1A. Biochim Biophys Acta 2017; 1860: 905–10
18. Lin Y, Wu Y, Li J, Dong C, Ye X, Chi YI, et al. The SNAG domain of Snail1 functions as a molecular hook for recruiting lysine-specific demethylase 1. EMBO J 2010; 29: 1803–16 [PubMed: 20389281]
19. Sheng W, LaFleur MW, Nguyen TH, Chen S, Chakravarthy A, Conway JR, et al. LSD1 Ablation Stimulates Anti-tumor Immunity and Enables Checkpoint Blockade. Cell 2018; 174: 549–63 e19 [PubMed: 29937226]
20. Qin Y, Vasilatos SN, Chen L, Wu H, Cao Z, Fu Y, et al. Inhibition of histone lysine-specific demethylase 1 elicits breast tumor immunity and enhances antitumor efficacy of immune checkpoint blockade. Oncogene 2019; 38: 390–405 [PubMed: 30111819]
21. Shi YJ, Matson C, Lan F, Iwase S, Baba T, Shi Y. Regulation of LSD1 histone demethylase activity by its associated factors. Molecular cell 2005; 19: 857–64 [PubMed: 16140033]
22. Wu Y, Wang Y, Yang XH, Kang T, Zhao Y, Wang C, et al. The deubiquitinase USP28 stabilizes LSD1 and confers stem-cell-like traits to breast cancer cells. Cell Rep 2013; 5: 224–36 [PubMed: 24075993]
23. Yi L, Cui Y, Xu Q, Jiang Y. Stabilization of LSD1 by deubiquitinating enzyme USP7 promotes glioblastoma cell tumorigenesis and metastasis through suppression of the p53 signaling pathway. Oncol Rep 2016; 36: 2935–45 [PubMed: 27632941]
24. Gong Z, Li A, Ding J, Li Q, Zhang L, Li Y, et al. OTUD7B Deubiquitinates LSD1 to Govern Its Binding Partner Specificity, Homeostasis, and Breast Cancer Metastasis. Advanced science (Weinheim, Baden-Wurttemberg, Germany) 2021; 8: e2004504 [PubMed: 34050636]
25. Chen BB, Mallampalli RK. F-box protein substrate recognition: a new insight. Cell Cycle 2013; 12: 1009–10 [PubMed: 23255120]
26. Skaar JR, Pagan JK, Pagano M. Mechanisms and function of substrate recruitment by F-box proteins. Nat Rev Mol Cell Biol 2013; 14: 369–81 [PubMed: 23657496]
27. Cenciarelli C, Chiaur DS, Guardavaccaro D, Parks W, Vidal M, Pagano M. Identification of a family of human F-box proteins. Curr Biol 1999; 9: 1177–9 [PubMed: 10531035]
28. Postow L, Funabiki H. An SCF complex containing Fbxl12 mediates DNA damage-induced Ku80 ubiquitylation. Cell Cycle 2013; 12: 587–95 [PubMed: 23324393]
29. Chen W, Gao D, Xie L, Wang A, Zhao H, Guo C, et al. SCF-FBXO24 regulates cell proliferation by mediating ubiquitination and degradation of PRMT6. Biochemical and biophysical research communications 2020; 530: 75–81 [PubMed: 32828318]
30. Wu Y, Evers BM, Zhou BP. Small C-terminal domain phosphatase enhances snail activity through dephosphorylation. The Journal of biological chemistry 2009; 284: 640–8 [PubMed: 19004823]
31. Wu Y, Wang Y, Lin Y, Liu Y, Wang Y, Jia J, et al. Dub3 inhibition suppresses breast cancer invasion and metastasis by promoting Snail1 degradation. Nature communications 2017; 8: 14228
32. Wu Y, Deng J, Rychahou PG, Qiu S, Evers BM, Zhou BP. Stabilization of snail by NF-kappaB is required for inflammation-induced cell migration and invasion. Cancer cell 2009; 15: 416–28 [PubMed: 19411070]
33. Dontu G, Abdallah WM, Foley JM, Jackson KW, Clarke MF, Kawamura MJ, et al. In vitro propagation and transcriptional profiling of human mammary stem/progenitor cells. Genes Dev 2003; 17: 1253–70 [PubMed: 12756227]
34. Qiu Z, Dong B, Guo W, Piotr R, Longmore G, Yang X, et al. STK39 promotes breast cancer invasion and metastasis by increasing SNAI1 activity upon phosphorylation. Theranostics 2021; 11: 7658–70 [PubMed: 34335956]
35. Dong C, Wu Y, Yao J, Wang Y, Yu Y, Rychahou PG, et al. G9a interacts with Snail and is critical for Snail-mediated E-cadherin repression in human breast cancer. J Clin Invest 2012; 122: 1469–86 [PubMed: 22406531]
36. Stavropoulos P, Blobel G, Hoelz A. Crystal structure and mechanism of human lysine-specific demethylase-1. Nat Struct Mol Biol 2006; 13: 626–32 [PubMed: 16799558]

37. Boulding T, McCuaig RD, Tan A, Hardy K, Wu F, Dunn J, et al. LSD1 activation promotes inducible EMT programs and modulates the tumour microenvironment in breast cancer. Sci Rep 2018; 8: 73 [PubMed: 29311580]
38. Hosseini A, Minucci S. A comprehensive review of lysine-specific demethylase 1 and its roles in cancer. Epigenomics 2017; 9: 1123–42 [PubMed: 28699367]
39. Han X, Gui B, Xiong C, Zhao L, Liang J, Sun L, et al. Destabilizing LSD1 by Jade-2 promotes neurogenesis: an antibraking system in neural development. Molecular cell 2014; 55: 482–94 [PubMed: 25018020]
40. Panchenko MV. Structure, function and regulation of jade family PHD finger 1 (JADE1). Gene 2016; 589: 1–11 [PubMed: 27155521]
41. Donner I, Kiviluoto T, Ristimaki A, Aaltonen LA, Vahteristo P. Exome sequencing reveals three novel candidate predisposition genes for diffuse gastric cancer. Fam Cancer 2015:
42. Bamford S, Dawson E, Forbes S, Clements J, Pettett R, Dogan A, et al. The COSMIC (Catalogue of Somatic Mutations in Cancer) database and website. Br J Cancer 2004; 91: 355–8 [PubMed: 15188009]
43. Nair VD, Ge Y, Balasubramaniyan N, Kim J, Okawa Y, Chikina M, et al. Involvement of histone demethylase LSD1 in short-time-scale gene expression changes during cell cycle progression in embryonic stem cells. Mol Cell Biol 2012; 32: 4861–76 [PubMed: 23028048]
44. Lv S, Bu W, Jiao H, Liu B, Zhu L, Zhao H, et al. LSD1 is required for chromosome segregation during mitosis. Eur J Cell Biol 2010; 89: 557–63 [PubMed: 20189264]
45. Cardozo T, Pagano M. The SCF ubiquitin ligase: insights into a molecular machine. Nat Rev Mol Cell Biol 2004; 5: 739–51 [PubMed: 15340381]
46. Michowski W, Chick JM, Chu C, Kolodziejczyk A, Wang Y, Suski JM, et al. Cdk1 Controls Global Epigenetic Landscape in Embryonic Stem Cells. Molecular cell 2020; 78: 459–76 e13 [PubMed: 32240602]
47. Chi Y, Carter JH, Swanger J, Mazin AV, Moritz RL, Clurman BE. A novel landscape of nuclear human CDK2 substrates revealed by in situ phosphorylation. Science advances 2020; 6: eaaz9899 [PubMed: 32494624]
48. Mosammaparast N, Kim H, Laurent B, Zhao Y, Lim HJ, Majid MC, et al. The histone demethylase LSD1/KDM1A promotes the DNA damage response. J Cell Biol 2013; 203: 457–70 [PubMed: 24217620]
49. Martin B, Chadwick W, Janssens J, Premont RT, Schmalzigaug R, Becker KG, et al. GIT2 Acts as a Systems-Level Coordinator of Neurometabolic Activity and Pathophysiological Aging. Front Endocrinol (Lausanne) 2015; 6: 191 [PubMed: 26834700]

Implications:

Our study provides comprehensive characterization of the significant role of FBXO24 in impeding breast tumor progression by targeting LSD1 for degradation.

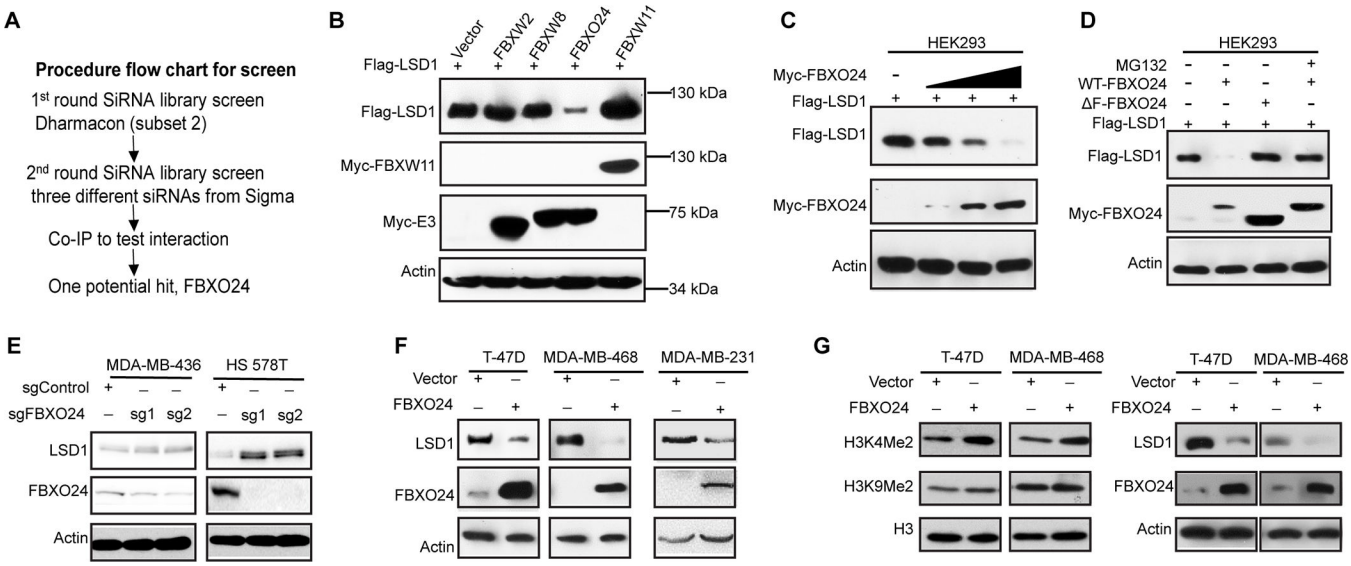

Figure 1. FBXO24 degrades LSD1.

(A) Experimental procedure flow chart for screen. **(B)** Flag-LSD1 was co-expressed with different E3 ligases in HEK293 cells and protein was detected by western blot. **(C)** LSD1 was co-expressed with increasing amounts of FBXO24. Lysates were subjected to western blot. **(D)** Flag-LSD1 was co-transfected with wild type (WT) or ΔF-FBXO24 (F-box domain deleted). Cells were treated with or without MG132. Expression of LSD1 and FBXO24 was assessed by western blot. **(E)** Immunoblot of lysates from cells with FBXO24 CRISPR knockout (SgRNA). **(F)** Immunoblot of lysates from FBXO24 overexpressing cells. **(G)** Acid extracted lysates were prepared to examine the histone markers by immunoblot (left). The expression of FBXO24 and LSD1 by western blot (right).

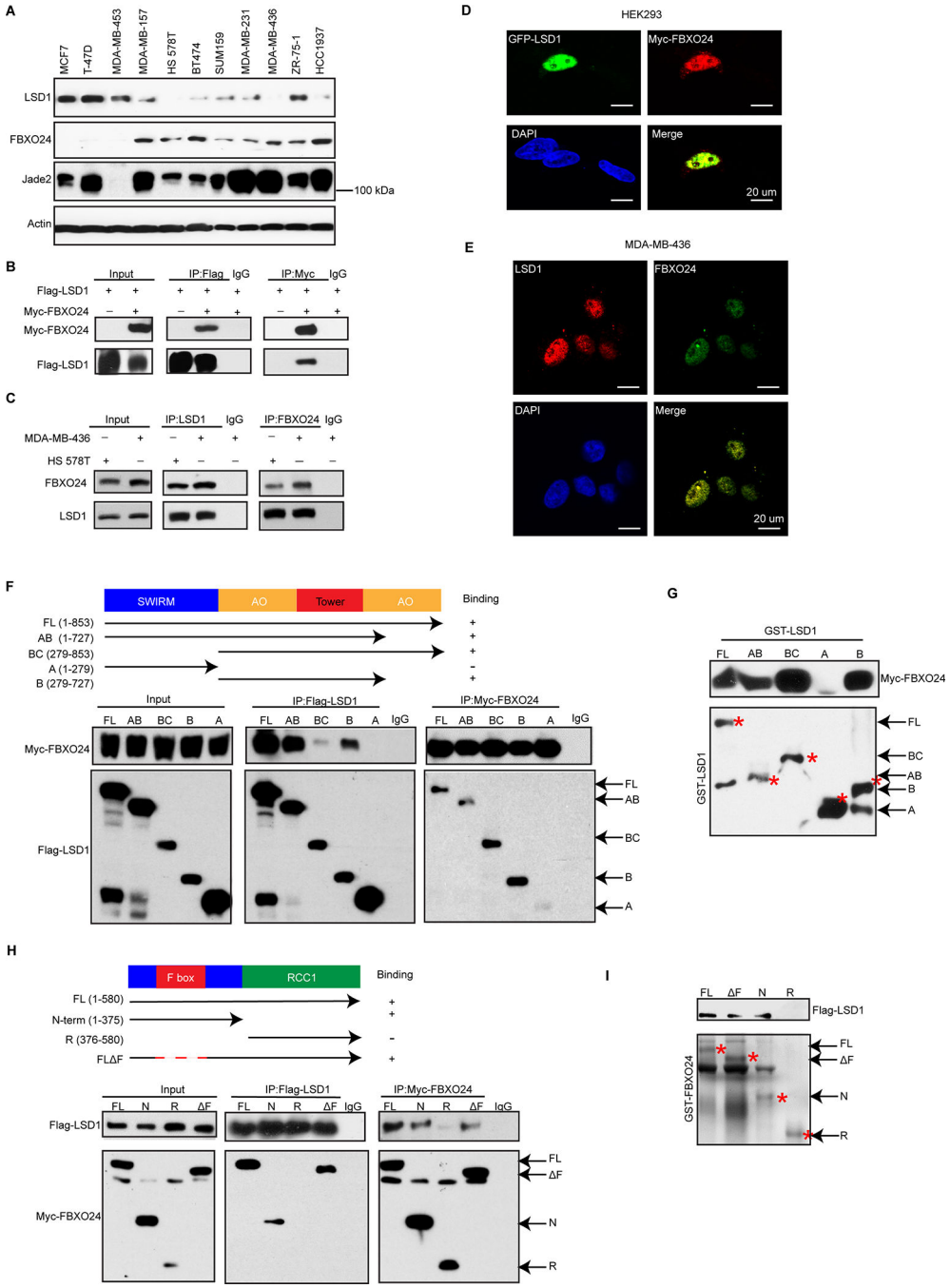

Figure 2. FBXO24 interacts and co-localizes with LSD1.

(A) Immunoblots of lysates from breast tumor cell lines. **(B)** Immunoblot of immunoprecipitation (IP) from HEK293 cells transfected with the indicated constructs. **(C)** Immunoblot of IP of endogenous FBXO24 or LSD1 in MDA-MB-436 and Hs 578T cells after treatment with MG132. **(D)** Confocal images of HEK293 cells co-expressing GFP-LSD1 with Myc-FBXO24 after treatment with MG132. **(E)** Confocal image of endogenous FBXO24 and LSD1 after treatment with MG132. **(F)** Schematic diagram showing the structure of LSD1 and deletion constructs used (top panel). Co-IP of exogenous Myc-

FBXO24 and Flag- full length (FL) LSD1 or different deletion mutants (lower panel). **(G)** Western blot analysis of Myc-FBXO24 pulled down by GST with full or different deletion mutants of LSD1. **(H)** Schematic diagram showing the structure of FBXO24 and deletion constructs used (top panel). Co-IP of exogenous Flag-LSD1 and Myc- full length (FL) FBXO24 or different deletion mutants (lower panel). **(I)** Western blot analysis of Flag-LSD1 pulled down by GST with full or different deletion mutants of FBXO24. Scale bar, 20 μm.

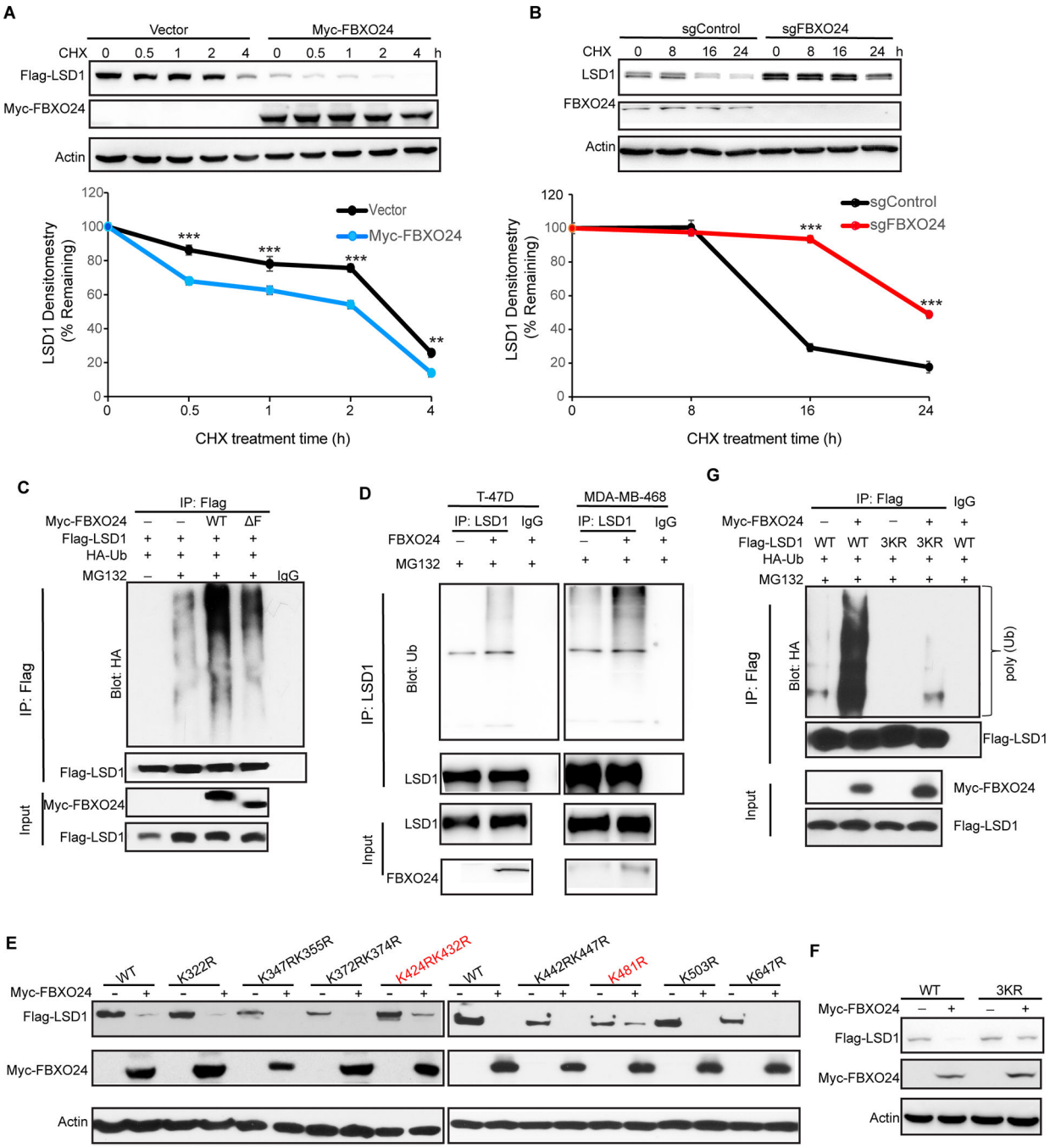

Figure 3. FBXO24 degrades LSD1 through ubiquitination.

A) Flag-LSD1 was co-expressed with vector or Myc-FBXO24 in HEK293 cells. After treatment with cycloheximide (CHX) for the indicated time intervals, expression of Flag-LSD1 and Myc-FBXO24 was analyzed by western blot using Flag and Myc antibodies, respectively. Presented data are representative of 3 separate experiments (up panel). The intensity of LSD1 expression for each time point was quantified by densitometry and plotted (low panel). **(B)** MDA-MB-436 cells were transfected with control or FBXO24 CRISPR knockout (SgRNA). After treatment with CHX as indicated above, expression

of endogenous LSD1 and FBXO24 was analyzed by western blot. Presented data are representative of 3 separate experiments (up panel). The intensity of LSD1 expression for each time point was quantified by densitometry and plotted (low panel). ** P<0.01, ***P<0.001, compared with controls. **(C)** Flag-LSD1 and HA-ubiquitin were co-expressed with WT or ΔF mutant FBXO24 in HEK293 cells. After treatment with 10 μM MG132 for 6 h, LSD1 was subjected to IP and the poly-ubiquitination of LSD1 assessed by western blot using HA antibody. IP LSD1 was probed using Flag antibody. Input protein levels of LSD1 and FBXO24 were examined using Flag and Myc antibodies, respectively. **(D)** T-47D and MDA-MB-468 cells stably transfected with vector, or FBXO24 were treated with MG132 for 6 h. Extracts were subjected to IP with LSD1 antibody and the poly-ubiquitination of LSD1 assessed by western blot using ubiquitin antibody. Input of LSD1 and FBXO24 were analyzed by western blot. **(E)** Myc-FBXO24 was co-expressed with Flag-tagged wild-type (WT) or different mutants of LSD1. Lysates were subjected to western blot. **(F)** Myc-FBXO24 was co-expressed with Flag-tagged wild-type (WT) or 3KR mutant of LSD1. Protein expressions of LSD1 and FBXO24 were analyzed by western blot. **(G)** Wild-type (WT) or 3KR mutant LSD1 and HA-ubiquitin were co-expressed with vector or FBXO24 in HEK293 cells. After treatment with 10 μM MG132 for 6 h, LSD1 was subjected to IP and the poly-ubiquitination of LSD1 assessed by western blot using HA antibody. IP LSD1 was probed using Flag antibody. Input protein levels of LSD1 and FBXO24 were examined using Flag and Myc antibodies, respectively.

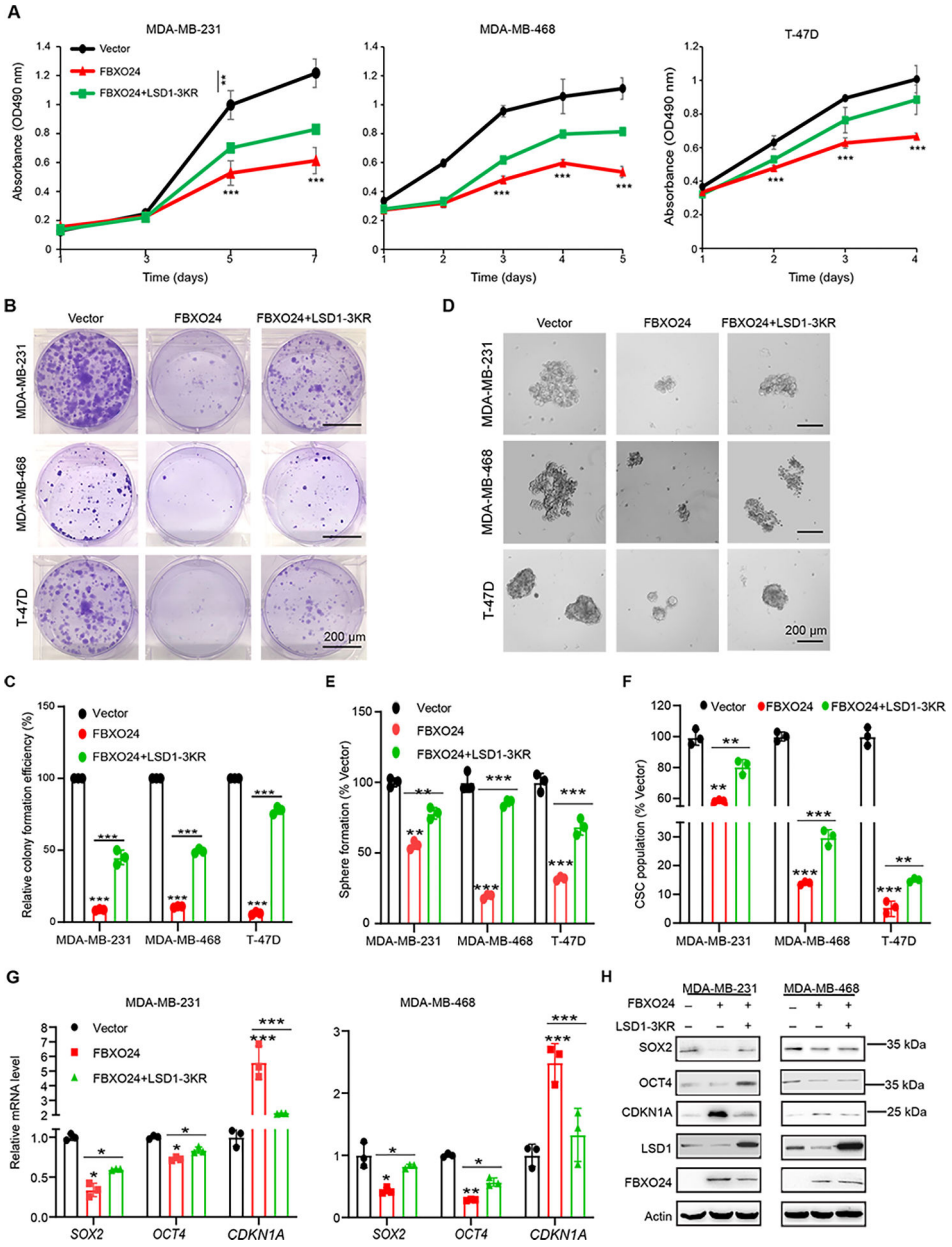

Figure 4. FBXO24 impairs tumor proliferation and CSC-like properties.

(A) Cell viability of FBXO24 or FBXO24+LSD1-3KR expressing MDA-MB-231, MDA-MB-468 and T-47D cells. **(B)** Representative images of colony formation in cells expressing FBXO24 with or without LSD1-3KR. **(C)** Graphic representation of (B). **(D)** Tumorsphere-formation was examined in MDA-MB-231, MDA-MB-468 and T-47D cells stably expressing vector, FBXO24 and FBXO24 with LSD1-rescued expression (LSD1-3KR). Representative images of primary tumorspheres from these cells were shown. **(E)** Quantification of tumorsphere from above experiments were plotted and shown. **(F)** $CD44^{high}/CD24^{low}$ population in cells above was examined by FACS analysis. **(G)** The mRNA levels were quantitated by real-time PCR. **(H)** Lysate from cells above were analyzed by western blot. *p<0.05, **p<0.01, and ***p value < 0.001 when control or

rescued group was compared with FBXO24 group (mean ± SD from three independent experiments). Scale bar, 200 μm.

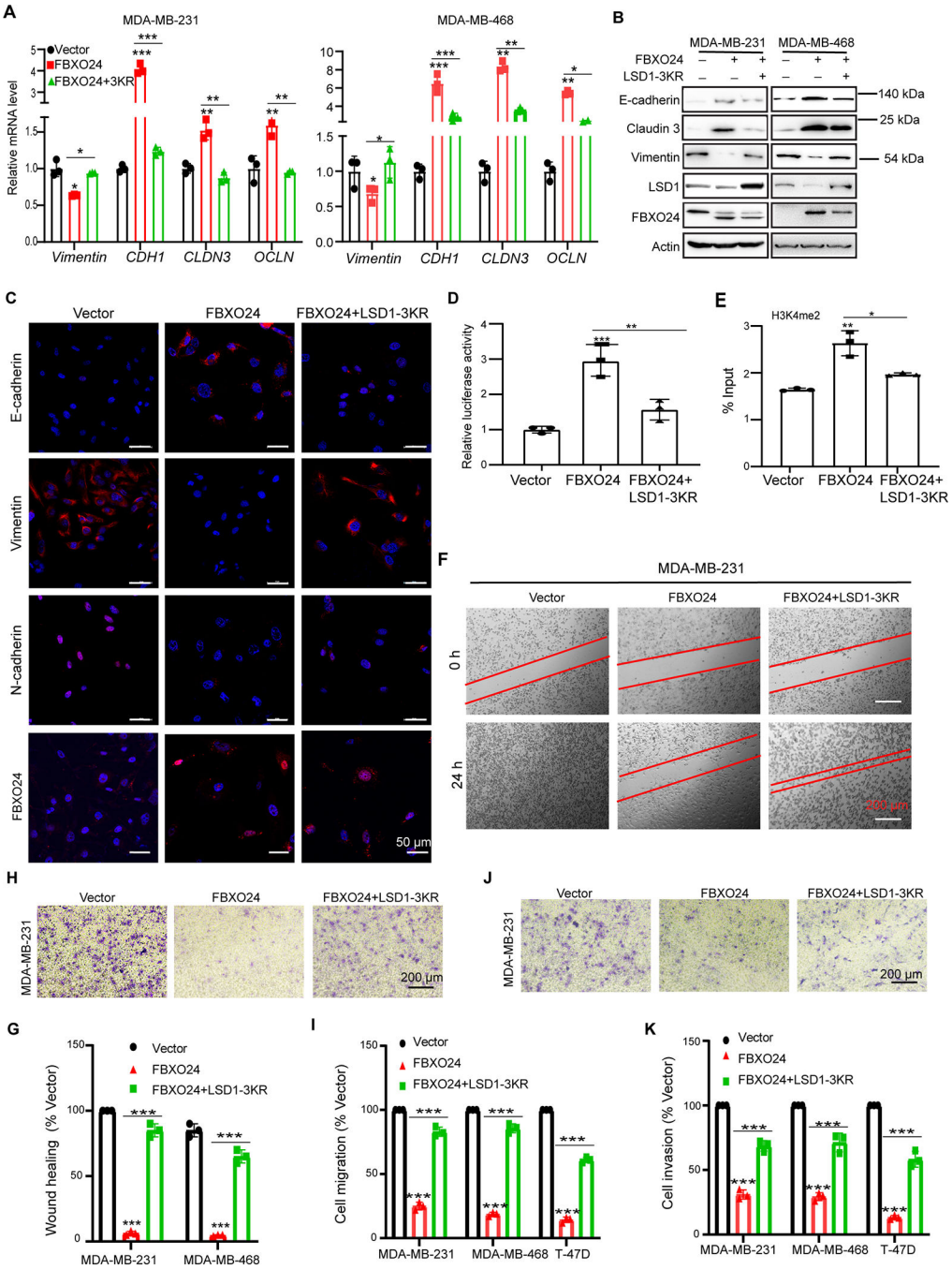

Figure 5. FBXO24 inhibits EMT and metastasis.

(A) The mRNA levels of EMT markers were quantitated by real-time PCR. CLDN3, Claudin 3; OCLN; Occludin. **(B)** The expression of E-cadherin, Claudin 3, Vimentin, LSD1, and FBXO24 was analyzed by western blot. (C) Immunofluorescent images of EMT markers in MDA-MB-231 cells. Scale bar, 50 μm**. (D)** The *CDH1* promoter reporter activity measured in MDA-MB-231 cells expressing vector, FBXO24 or FBXO24+LSD1-3KR. **(E)** ChIP-qPCR analysis of the occupancy of *CDH1* using H3K4me2 antibody in above cells. **(F)** Representative phase-contrast microscope images showing the area covered by

the cells at 0 and 24 h after wounding in MDA-MB-231 cells. **(G)** Graphic representation of wound-healing closure described in (F). **(H)** Representative images of Boyden chamber migration assay of modified MDA-MB-231 cells transfecting with vector, FBXO24 or FBXO24+LSD1-3KR. **(I)** Graphic representation of cell motility described in (H) analyzed by a migration assay. **(J)** Representative images of Boyden chamber invasion assay of modified MDA-MB-231 cells. **(K)** Graphic representation of cell invasion described in (J). *p<0.05, **p<0.01, and ***p value < 0.001 when control or rescued group was compared with FBXO24 (group mean ± SD from three independent experiments). Scale bars, 200 μm.

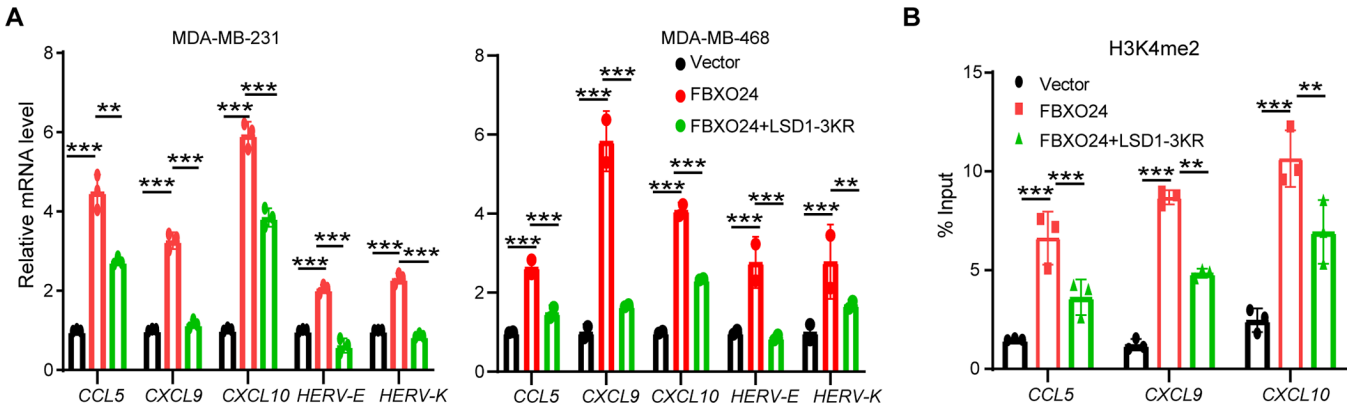

Figure 6. FBXO24 promotes expression of ERV and chemokines.

(A) The mRNA levels of chemokine and endogenous retroviral elements (ERV) were quantitated by real-time PCR. **(B)** ChIP-qPCR analysis of the occupancy of chemokines using H3K4me2 antibody in MDA-MB-231 cells expressing vector, FBXO24 or FBXO24+LSD1-3KR. *p<0.05, **p<0.01, and ***p value < 0.001 when control or rescued group was compared with FBXO24 (group mean ± SD from three independent experiments)

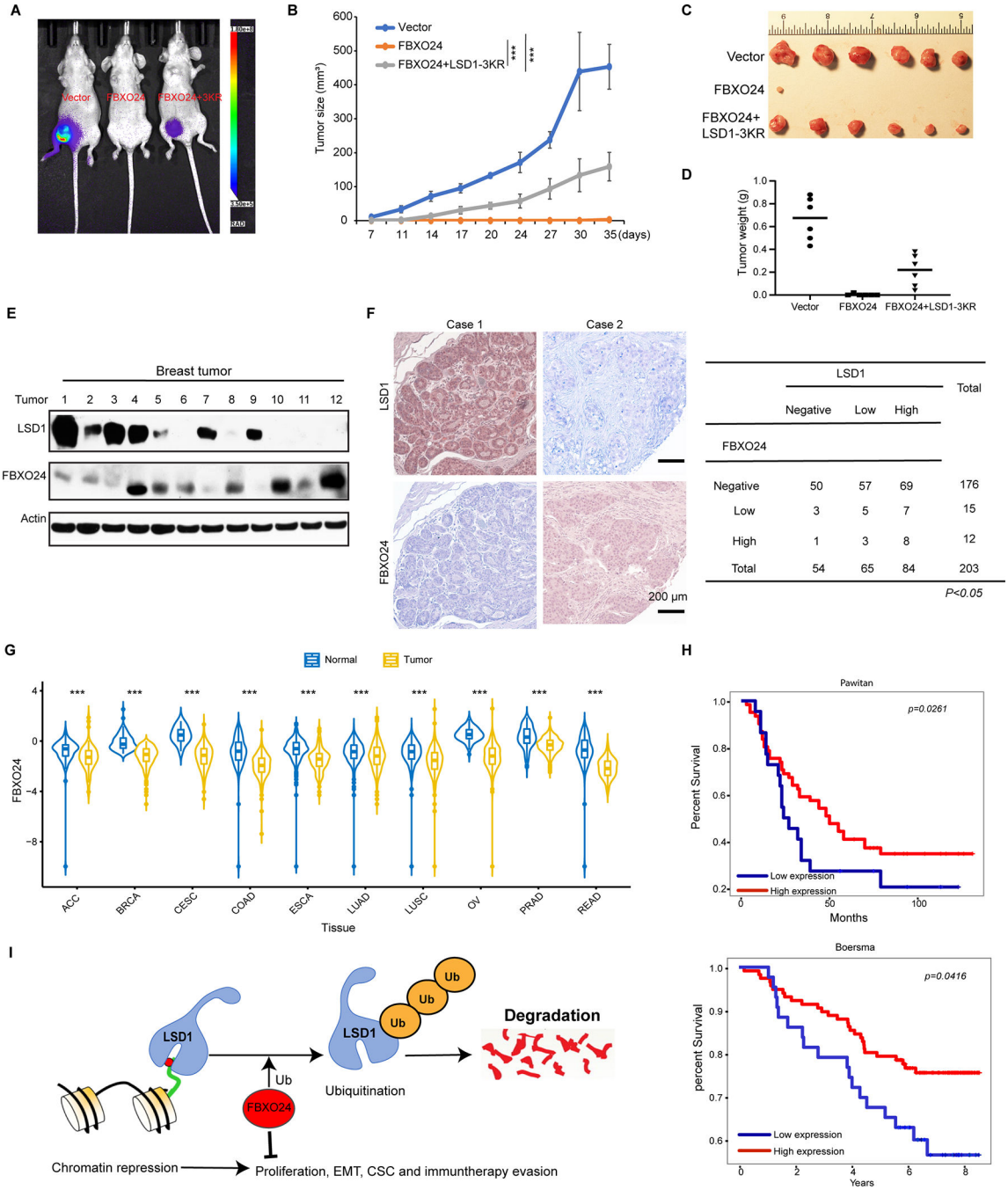

Figure 7. FBXO24 represses tumor growth and negatively associates with LSD1 in breast cancer samples.

(A-D) MDA-MB231-luc cells were injected into the mammary fat pad of SCID mice (n=6). Tumor size was recorded by bioluminescence imaging (A). Tumor growth curve (B), photographs of harvested tumors (C), and tumor weights (D) were measured. **(E)** Expression of FBXO24 and LSD1 from 12 cases of fresh frozen human breast tumors was examined by western blot. **(F)** The 203 surgical specimens of breast cancer were immunostained using antibodies against LSD1 and FBXO24. Representative images of IHC

analysis for LSD1 and FBXO24 in the serial sections of tumor tissues (left panel). Statistical analysis is shown in right table. **(G)** Violin plot showing z-scores of FBXO24 mRNA expression in tumor and normal tissues in TCGA cancer dataset. ACC, Adrenocortical carcinoma; BRCA, Breast invasive carcinoma; CESC, Cervical Squamous Cell Carcinoma and Endocervical Adenocarcinoma; COAD, Colon Adenocarcinoma; ESCA, Esophageal Carcinoma; LUAD, lung adenocarcinoma; LUSC, lung squamous cell carcinoma; OV, Ovarian serous cystadenocarcinoma; PRAD, Prostate Adenocarcinoma; READ, Rectum Adenocarcinoma. **(H)** Kaplan–Meier plots of survival of patients, stratified by expression of FBXO24. Data obtained from the Pawitan and Boersma database. P-values represent log-rank testing of the difference in cumulative survival. **(I)** A proposed model to illustrate FBXO24 induces LSD1 degradation through a ubiquitination event. ***p value < 0.001. Scale bars, 200 μm.